

# Solvation of the Menshutkin Reaction: A Rigorous Test of the Effective Fragment Method

Simon P. Webb and Mark S. Gordon\*

Department of Chemistry, Iowa State University, Ames, Iowa 50011

Received: September 18, 1998; In Final Form: December 4, 1998

The recently developed effective fragment potential (EFP) method is used to study the effect of two, four, six, and eight solvating water molecules on the Menshutkin reaction between ammonia and methyl bromide. The EFP method reproduces all *ab initio* geometries and energetics (including zero-point energy, thermal, and entropy effects) for the two-water case very accurately. Energetics from all *ab initio* single-point energies at the EFP geometries for the four, six, and eight water cases are in excellent agreement with corresponding EFP energetics. In the gas phase, the above Menshutkin reaction is kinetically highly unfavorable with a free energy of activation (at 298.15 K) of 40.6 kcal/mol at the RHF level with a double- $\xi$  basis set augmented with polarization and diffuse functions. An ion-pair product is found, in agreement with previous work, in which the bromide anion is hydrogen-bonded to an ammonium hydrogen, giving a free energy of reaction of 2.8 kcal/mol. The addition of solvating water molecules has the effect of lowering the barrier and lowering the energy of the ion-pair product relative to the molecule-pair reactant. For eight solvating EFP water molecules, the free energy of activation is 22.8 kcal/mol and the free energy of reaction is  $-21.9$  kcal/mol. Timings indicate that the EFP method allows the inexpensive addition of water molecules to a chemical system, accurately modeling all *ab initio* calculations with low computational cost.

## I. Introduction

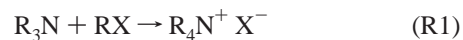
Modeling of solvation effects is one of the great challenges in computational chemistry. Continuum-based methods<sup>1</sup> are widely used and are becoming increasingly sophisticated. Some of these methods now employ variable cavity shapes produced by a union of spheres centered on each atom of the solute and account for effects such as cavitation energy, dispersion, and repulsion.<sup>2</sup> The continuum approach has proved to be very important. Even the simplest single-sphere self-consistent reaction field method has provided useful information concerning solvent effects on suitable systems.<sup>3</sup> The more sophisticated methods are able to handle a wide range of molecules and reactions.<sup>4</sup> However, continuum methods are unable to identify the role of individual solvent molecules in the solvation process, thereby precluding detailed analysis of the mechanism of solvation in the systems under study.

Another approach to the solvation problem has been to characterize the *ab initio* gas phase potential energy surface and then introduce discrete *ab initio* waters one at a time forming a supermolecule. While this approach has yielded fundamental information on the solvation process<sup>5</sup> it quickly becomes prohibitively expensive if more than a handful of solvent molecules are included. The importance of the discrete solvent molecule approach is reflected in the development and increasing popularity of hybrid QM/MM methods which treat the solute with *ab initio* or semiempirical techniques and the solvent molecules with cheaper molecular mechanics force fields.<sup>6</sup>

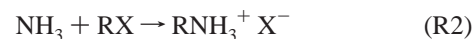
The effective fragment potential (EFP) method,<sup>7,8</sup> developed in this laboratory, accounts for solvent effects on chemical reactions by treating solute molecules fully *ab initio* and introducing discrete solvent molecules through potentials added as one-electron terms directly into the *ab initio* Hamiltonian. In the current implementation for aqueous solution the potentials are derived directly from separate *ab initio* calculations on water and water dimer. It has recently been demonstrated that the EFP

method accurately reproduces RHF structures and relative energetics for small water clusters.<sup>9</sup> It has previously been shown that the EFP method can reproduce all *ab initio* RHF relative energies and geometries in a study on the internal rotation in ground state formamide with up to five waters.<sup>10</sup> It has also successfully reproduced the results of all *ab initio* MCSCF calculations on excited state formamide with two water molecules.<sup>11</sup> Day and Pachter have reported results of a study on aqueous glutamic acid, using the EFP method to model the effects of up to 10 water molecules.<sup>12</sup> In this paper, we further test the EFP method by its application to the Menshutkin reaction.<sup>13</sup> This reaction, in which neutral reactants lead to separated ion products, is the most stringent test of the method to date.

In 1890 Menshutkin studied the reaction between the alkyl amines and alkyl halides (R1).



He found that the reaction rate increases dramatically when the polarity of the solvent is increased.<sup>13</sup> This increase in reaction rate with solvent polarity is attributed to the stabilization of the reaction path to ion separation, by the solvent. The reaction (R2) between ammonia and alkyl halide



is an example of a Menshutkin reaction and is an intermediate step in the formation of primary amines.<sup>14</sup> Investigating the effect of solvation on the Menshutkin reaction is important in terms of understanding the fundamental process of solvation of ion formation. Consequently, there have been a number of theoretical investigations of the solvent effect on this reaction.

Solà et al. have studied the reaction between ammonia and methyl bromide, reporting relative energies calculated at the

RHF/3-21G level of theory (no zero-point energy (ZPE) or temperature effects).<sup>15</sup> In the gas phase the reactants were found to form a so-called "ion-pair reactant" which lies in a shallow well (−2.8 kcal/mol relative to separated reactants). Subsequently, we will refer to this reactant complex as a "molecule-pair reactant". The transition state is found to be high in energy (23.3 kcal/mol relative to separated reactants), leading to an "ion-pair product" which lies in a shallow well (20.7 kcal/mol relative to separated reactants), and finally highly unstable separated products are predicted (103.8 kcal/mol relative to separated reactants). These authors introduced discrete solvent molecule effects by addition of two *ab initio* waters, and in separate calculations they modeled the bulk effects of water, methanol, and hexane using a continuum method.<sup>2</sup> The addition of two discrete waters, one associated with the NH<sub>3</sub> group and the other with the Br, resulted in an earlier and lower energy transition state (10.8 kcal/mol relative to separated reactants), and stabilized the ion-pair product (−0.2 kcal/mol relative to separated reactants) and the separated ions (59.2 kcal/mol relative to separated reactants), with the overall process remaining endothermic. The continuum model gives a barrier of 8.3 kcal/mol for the hydrated reaction and predicts the separated products to be stable with respect to reactants by 44.0 kcal/mol. With hexane as the solvent, formation of a molecule-pair reactant and ion-pair product is predicted (−2.2 kcal/mol and −5.7 kcal/mol, respectively, relative to separated reactants), along with a high-energy transition state (14.5 kcal/mol) and endothermic final product ions (23.6 kcal/mol), illustrating the effect of solvent polarity.

Gao and Xia used a QM/MM approach in statistical mechanical Monte Carlo simulations to study the ammonia–methyl chloride Menshutkin reaction in aqueous solution.<sup>16</sup> The solute is modeled using the semiempirical AM1 method and the 256 solvent water molecules by the TIP3P potential.<sup>17</sup> The predicted free energy of activation at 298.15 K is  $26.3 \pm 0.3$  kcal/mol which the authors compare with the experimental activation energy of 23.5 kcal/mol for the related iodide system.<sup>18</sup> Gao et al. contend that the large discrepancy between their predicted barrier height and that of Solà et al. suggests that the description of discrete solute–solvent interactions is necessary in this system, though basis set, ZPE, thermal, and entropy effects need to be considered. For the reaction free energy Gao et al. predict −18 kcal/mol, indicating a thermodynamically favorable reaction in aqueous solution.

Recently, Truong et al. have carried out a study of the free energy profile of the ammonia–methyl chloride Menshutkin reaction in aqueous solution using the continuum method GCOSMO.<sup>4b</sup> They predict a free energy of activation of 24.8 kcal/mol and a reaction free energy of −16.5 kcal/mol and so are in good agreement with the QM/MM study of Gao et al.

Maran, Pakkanen, and Karelson<sup>19</sup> have studied the reaction between ammonia and the alkyl halides—methyl chloride, methyl bromide, and methyl iodide, using the semiempirical method AM1 and describing solvent effects (water and hexane) through a multicavity self-consistent reaction field method. Their calculated barrier (no temperature effects included) for the chloride, bromide, and iodide aqueous systems are 21, 25, and 37 kcal/mol, respectively. More recently, the same authors have carried out *ab initio* calculations to examine in detail just the gas phase reactions.<sup>20</sup>

In this paper, we report results of a study in which we apply the EFP method to microsolvation of the reaction between ammonia and methyl bromide.



Our main objective is to test the performance of the EFP method. We examine the EFP method's accuracy and relative expense by comparison to all *ab initio* calculations and also explore the effects of selected arrangements of 0–8 water molecules on the reaction profile. In addition, we examine ZPE effects as well as thermal and entropy effects at room temperature for the zero, two, and eight water cases.

## II. Computational Details

The gas phase potential energy surface of the reaction between ammonia and methyl bromide was explored using restricted Hartree–Fock (RHF) and second-order perturbation theory (MP2)<sup>21</sup> geometry optimization methods. For solvated systems, only RHF calculations were carried out. Characterization of all stationary points was achieved by calculating and diagonalizing the energy second derivative matrix (Hessian). A positive definite Hessian (no negative eigenvalues) indicates a minimum on the potential energy surface; one negative eigenvalue indicates a transition state.

For hydrogen, carbon, nitrogen, and oxygen, the double- $\xi$  basis set of Dunning and Hay<sup>22</sup> was used; for bromine the double- $\xi$  basis of Binning and Curtiss was employed.<sup>23</sup> P polarization functions were added to hydrogens, and d polarization functions were added to all heavy atoms. A diffuse sp shell was also added to bromine. Exponents used are the defaults in GAMESS.<sup>24</sup> Collectively this basis set is referred to as DZVP.

Water molecules were added to the system through use of the effective fragment potential (EFP) method.<sup>7,8</sup> The method is described in detail in a previous paper,<sup>8</sup> and a summary is given in an application to the solvated internal rotation of formamide.<sup>10</sup> Also summarized in the latter paper are the geometry search procedure, and the intrinsic reaction coordinate (IRC) procedure<sup>25</sup> which follows the minimum energy path (MEP) from transition states to minima. Both techniques were utilized in this study. Numeric calculation of the Hessian was carried out through double displacements of the stationary point geometries and analytic calculation of the energy gradients.

For comparison, *ab initio* waters were added in a supermolecule approach. For the two-water system all *ab initio* geometry optimizations and Hessians were done to test the accuracy of the EFP geometries, relative energies, and calculated frequencies. For larger numbers of waters (4–8) all *ab initio* single-point energy calculations at EFP geometries were performed to test relative energies.

Zero-point energy (ZPE) corrections and thermochemical quantities were calculated using the harmonic mode, ideal gas, and rigid rotator approximations. The Hessian matrix does not include internal vibrations of EFP waters. These vibrations are therefore omitted from ZPE and thermochemical contributions to enthalpy and entropy (and consequently to free energy) in calculations with EFP waters.

## III. Results and Discussion

**(a) Gas Phase Surface.** In order to establish a point of reference, we first explore and characterize the gas phase potential energy surface of the reaction between ammonia and methyl bromide. Results of RHF/DZVP and MP2/DZVP geometry searches are presented in Figures 1 and 2, and Table 1. Energies discussed in this and other sections of the paper, unless otherwise stated, will be  $\Delta E$ s, that is, relative energies with no ZPE or temperature effects included. The minimum

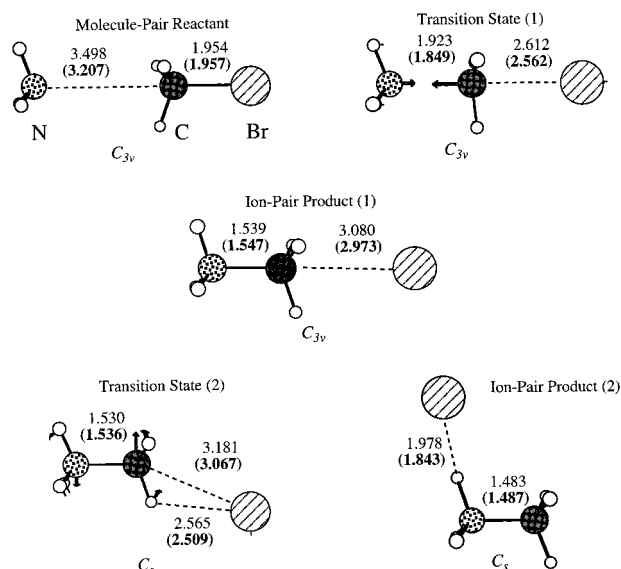


**Figure 1.** RHF/DZVP and MP2/DZVP optimized stationary point structures on the potential energy surface of the Menshutkin reaction (R3) in the gas phase. Bond lengths are in angstroms. MP2 bond lengths are in bold type and in parentheses. Arrows in transition states indicate displacements in the imaginary normal mode.

energy path, determined by the IRC procedure,<sup>25</sup> linking the molecule-pair reactant with transition states and ion-pair products is shown in Figure 3.

The first part of the surface, that is, the molecule-pair reactant, transition state (1), and ion-pair product (1), is qualitatively the same as that predicted by Solà et al.<sup>15</sup> However, Table 1 shows some quantitative discrepancies. The molecule-pair reactant to transition state barrier is found to be  $\sim 10$  kcal/mol higher than that in the earlier study. The relative RHF/DZVP energy of the transition state and ion-pair product agrees closely with the earlier work (8.4 kcal/mol compared to 8.9 kcal/mol). Consequently, the ion-pair product itself is predicted to be  $\sim 10$  kcal/mol less stable (relative to separated reactants) than predicted by Solà et al. Tests done during the course of this study show that the small size of the underlying 3-21G basis set used by Solà is the main source of these energy discrepancies. This is confirmed below via comparison with results from calculations<sup>20</sup> with basis sets more comparable in quality to those used in the present study. Inclusion of polarization and diffuse functions is found to make a considerable difference to predicted geometries, but the effect on relative energies is found to be small.

Dynamic electron correlation introduced through MP2 does result in some contraction in bond lengths, but makes little difference to the energetics. Therefore, RHF is considered adequate for study of the solvated system. Mulliken populations (see Table 2), while not meaningful in an absolute sense, do show that the Br accumulates charge as the reaction proceeds through the first transition state. It has acquired a charge of  $\sim -0.9$  in the ion-pair product (1).

Normally, from the ion-pair product the potential energy surface is assumed to proceed directly to the highly energetic separated products:  $\text{CH}_3\text{NH}_3^+ + \text{Br}^-$ ; however, Maran et al.<sup>20</sup> recently discovered a second ion-pair product, at the RHF, CISD, MP2, and MP3 levels, using a 6-31G\* basis set, with the  $\text{Br}^-$  directly interacting with an  $\text{NH}_3$  hydrogen via a hydrogen bond. This latter species is predicted to be lower in energy than separated reactants. We also consider this species in which the bromide is weakly bound to an  $\text{NH}_3$  hydrogen. Figure 2 and Table 1 show that there is a very small barrier of 0.3 kcal/mol

at the RHF/DZVP level of theory leading from the  $C_{3v}$  ion-pair product to a  $C_s$  transition state (Figure 3 indicates that this is little more than a shoulder on the PES) in which the Br has moved in toward a hydrogen. This transition state leads to a  $C_s$  minimum, described above, which is lower in energy than separated reactants by 6.5 kcal/mol at the RHF/DZVP level of theory. The separated products lie 105.9 kcal/mol above this minimum. Dynamic electron correlation effects on relative energies are more pronounced in this region of the surface with an increase in energy of  $\sim 3$  kcal/mol for the  $C_{3v}$  ion-pair product– $C_s$  transition state barrier and a decrease in energy of  $\sim 5$  kcal/mol for the  $C_s$  ion-pair product due to the MP2 correction.

However, RHF still provides a reasonable description of the process. Mulliken populations (see Table 2) indicate that the charge on the Br is lowered considerably on formation of the second ion-pair product due to the formation of the strong  $\text{Br} \cdots \text{H}-\text{N}$  hydrogen bond.

The RHF and MP2 energetics calculated in this study (Table 1) and those from Maran, Karelson, and Pakkanen<sup>20</sup> are in reasonable agreement. They predict a first transition state at 30.8 and 30.3 kcal/mol relative to the molecule-pair reactant at RHF/6-31G\* and MP2/6-31G\*, respectively. For the second ion-pair product they predict  $-6.5$  and  $-8.8$  kcal/mol relative to the molecule-pair reactant at RHF/6-31G\* and MP2/6-31G\*, respectively. Our results for this particular Menshutkin reaction (R3) confirm their conclusion that the gas phase reaction to form the ion-pair product (2) (see Figure 2) is energetically favorable (by 6.5 kcal/mol using RHF/DZVP) but there exists a very high barrier (34.0 kcal/mol with RHF/DZVP) to overcome in order for the reaction to proceed. If ZPE corrections are included, as well as thermal and entropy effects at 298.15 K (Table 4) the free-energy of activation is 40.6 kcal/mol and the free-energy of reaction forming the ion-pair product (2) is 2.8 kcal/mol, so overall these effects clearly favor the reactant complex.

**(b) Two Waters.** Next, two *ab initio* waters were introduced. No symmetry constraints were placed on the system during the geometry optimizations. Figure 4 and Table 3 show the structures and relative energies of what were found to be lowest energy species on the potential energy surface. The structures were found by first identifying the lowest energy transition state with two water molecules and then performing IRC calculations<sup>10,25</sup> by stepping forward and backward from the transition state along the imaginary mode leading to reactant and product minima. Also shown in Figure 4 and Table 3 are the corresponding structures and energetics from calculations with the two *ab initio* waters replaced by two EFP waters. The EFP method is found to do an excellent job of reproducing the all *ab initio* results. All EFP bond lengths are within 0.06 Å of those predicted *ab initio* and most agree much more closely than this upper bound. EFP relative energies are found to agree with the all *ab initio* relative energies to within 0.3 kcal/mol. The EFP and *ab initio* imaginary frequency at the transition state are also in excellent agreement.

The effect of two water molecules is found to be dramatic (see Table 3). The barrier from molecule-pair reactant to transition state is lowered by 11.8 kcal/mol to a value of 22.2 kcal/mol and the ion-pair product is now lower in energy than the molecule-pair reactant by 19.2 kcal/mol. The transition state geometry (see Figure 4) shows that it is occurring earlier in the reaction, an effect also observed in previous studies<sup>15</sup> and predicted by the Hammond postulate.

Figure 5 shows the all *ab initio* and the two EFP water minimum energy paths (MEPs). Both curves are relative to their



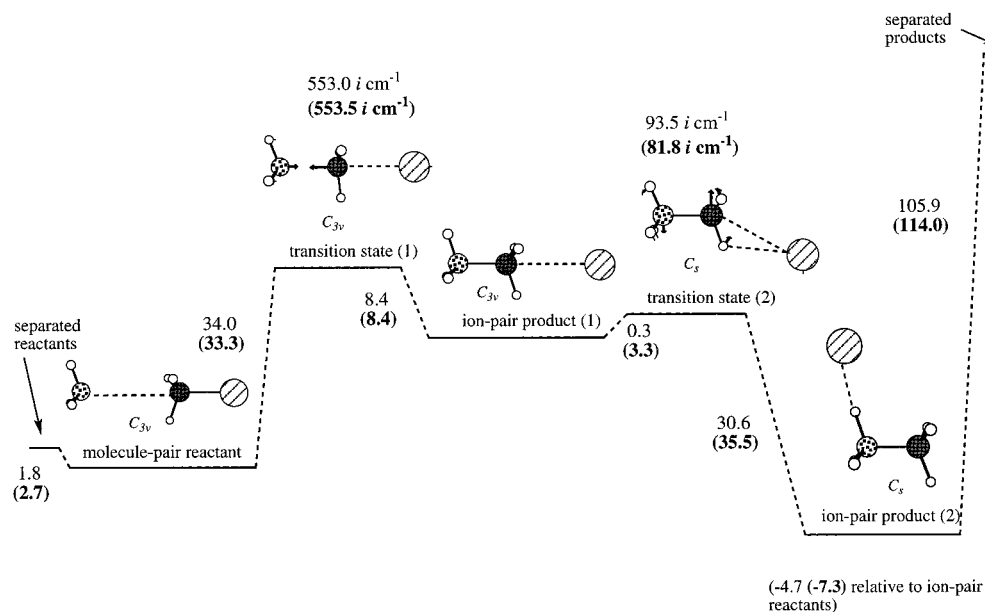


**Figure 2.** RHF/DZVP and MP2/DZVP potential energy surfaces of the Menshutkin reaction (R3) in the gas phase at 0 K (no ZPE corrections). Energies are in kcal/mol. Harmonic vibrational frequencies and displacements (see arrows) are shown for transition states. Diagram is not to scale. MP2/DZVP values are in bold type.

**TABLE 1: Calculated Energies (in kcal/mol) Relative to the Molecule-Pair Reactant for the Menshutkin Reaction (R3) in the Gas Phase at 0 K**

	RHF/DZVP <sup>a</sup>		MP2/DZVP <sup>a</sup>	
	$\Delta E$	$\Delta H$ (0 K) <sup>b</sup>	$\Delta E$	$\Delta H$ (0 K) <sup>b</sup>
separated reactants	1.8	1.2	2.7	2.0
molecule-pair reactant	0.0	0.0	0.0	0.0
transition state (1)	34.0	36.2	33.0	35.0
ion-pair product (1)	25.6	30.2	24.9	28.7
transition state (2)	25.9	30.5	28.2	32.1
ion-pair product (2)	-4.7	-0.6	-7.3	-4.9
separated ion products	101.2	105.3	106.6	110.8

<sup>a</sup> Geometry is optimized at this level of theory. <sup>b</sup> Calculated relative energy,  $\Delta E$ , plus ZPE correction.

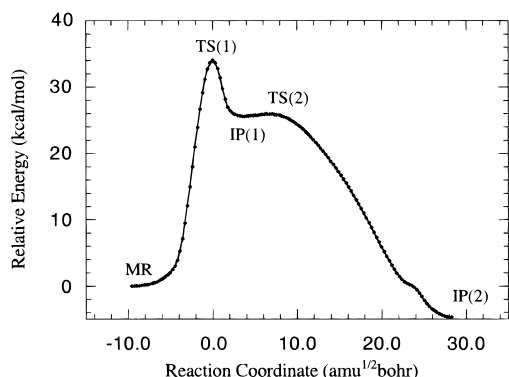


**Figure 3.** Minimum energy path for the gas phase Menshutkin reaction (R3). Energy points are in kcal/mol and are relative to the ion-pair reactants. MR = molecule-pair reactant, TS(1) = first transition state, IP(1) = first ion-pair product, TS(2) = second transition state, IP(2) = second ion-pair product: see Figure 2.

respective molecule-pair reactant minimum. The EFP MEP does not go to zero at its end point, indicating that it is in a shallow well just above the true minimum. The two MEPs map onto each other very closely up through the transition state but diverge by up to  $\sim 5$  kcal/mol on the part of the surface representing the migration of the bromide anion. However, these MEPs nearly merge again at the ion-pair product structures.

The MEPs for the two water molecule case (see Figure 5)

**TABLE 2: RHF/DZVP Mulliken Charges for Stationary Points on the Potential Energy Surface of the Menshutkin Reaction (R3) in the Gas Phase**

	Mulliken charges				
	NH <sub>3</sub>		CH <sub>3</sub>		
	N	H	C	H	Br
separated reactants	-0.747	0.249	-0.283	0.158	-0.193
ion-pair reactant	-0.758	0.255	-0.251	0.158	-0.229
transition state (1)	-0.730	0.319	-0.169	0.225	-0.739
ion-pair product (1)	-0.524	0.352	-0.272	0.219	-0.918
transition state (2)	-0.512	0.357 ( $\times 2$ )	-0.251	0.191 ( $\times 2$ )	-0.928
ion-pair product (2)	-0.441	0.328 ( $\times 2$ )	-0.253	0.186 ( $\times 2$ )	-0.780
separated ion products	-0.478	0.375	-0.248	0.201	-1.000

show that two waters are sufficient to produce a low energy ( $-19.2$  kcal/mol relative to the molecule-pair reactants) ion-pair product complex directly. Inspection of the ion-pair product structure (see Figure 4) reveals that the MEP from the transition state leads directly to the arrangement seen in the gas phase (the migration mentioned above), with the bromide hydrogen-bonded to an ammonium hydrogen. The presence of the two waters has removed the small barrier to this process found in the gas phase. The low energy of the ion-pair product solvated with two waters, then, is partly due to the same effect seen in the gas phase and partly due to the hydrogen-bonding of the waters to the charged bromide and ammonium hydrogen. Table 4 shows that the introduction of ZPE, as well as thermal and entropy effects at 298.15 K increases the barrier by 6.6 kcal/mol leading to a free energy of activation of 28.3 kcal/mol and increases the energy of the ion-pair product by 7.5 kcal/mol making the free-energy of reaction  $-10.2$  kcal/mol. The EFP calculations reproduce these effects extremely well giving 27.7 and  $-10.3$  kcal/mol for the corresponding free energies. Again, overall these effects favor the reactant complex.

**(c) Four and Six Waters.** Having shown that the EFP method reproduces all *ab initio* geometries to a high degree of accuracy, geometry optimizations and IRC calculations with additional water molecules have been performed only with the EFP method.

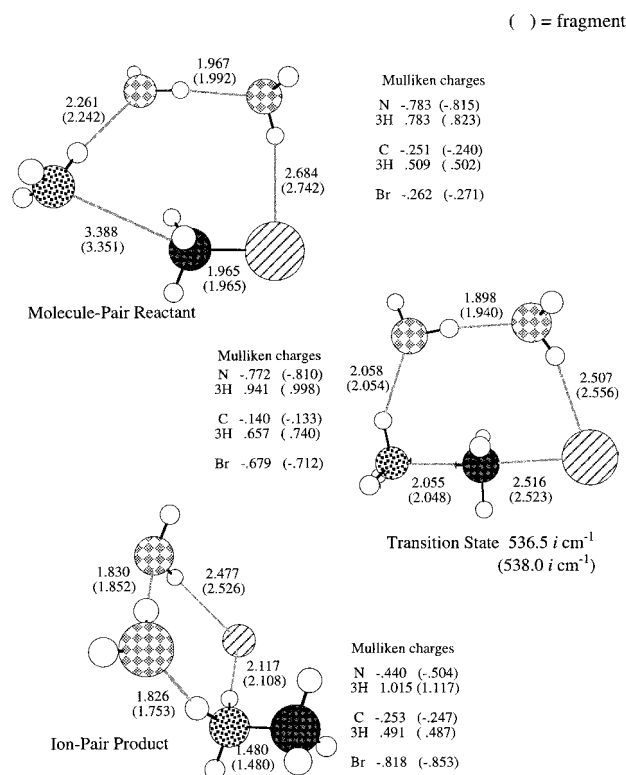


**Figure 4.** RHF/DZVP all *ab initio* structures and Mulliken charges for the Menshutkin reaction (R3) with two water molecules and the corresponding structures and charges with two EFP waters. Bond lengths are in angstroms. Parentheses indicate EFP method. Arrows in transition states indicate displacements in the imaginary normal mode.

**TABLE 3: Calculated Energies (kcal/mol) at 0 K, Relative to the Lowest Energy Molecule-Pair Reactant in the Menshutkin Reaction (R3) with 0, 2, 4, 6, and 8 Solvating Water Molecules<sup>a</sup>**

no. of waters		$\Delta E$ /kcal/mol	
		EFP	ab initio
0	M-P React.		0.0
	T.S.(1)		34.0
	I-P Prod.(2)		-4.7
2 <sup>b</sup>	M-P React.	0.0	0.0
	T.S.	22.5	22.2
	I-P Prod.	-19.4	-19.2
4 <sup>c</sup>	symmetric	M-P React.	3.9 (0.0) <sup>d</sup>
		T.S.	17.6 (13.7) <sup>d</sup>
		I-P Prod.	-30.7 (-34.6) <sup>d</sup>
	nonsymmetric	M-P React.	0.0
		T.S.	18.0
		I-P Prod.	-26.2
6 <sup>c</sup>	symmetric	M-P React.	0.9 (0.0) <sup>d</sup>
		T.S.	23.0 (22.1) <sup>d</sup>
		I-P Prod.	-19.7 (-20.6) <sup>d</sup>
	nonsymmetric	M-P React.	0.0
		T.S.	16.0
		I-P Prod.	-29.1
8 <sup>c</sup>	M-P React.	0.0	0.0
	T.S.	20.9	19.9
	I-P Prod.	-30.9	-30.8

<sup>a</sup> Zero-point energies and temperature effects are not included. <sup>b</sup> Both EFP and all *ab initio* energies from fully optimized structures. <sup>c</sup> EFP energies are from fully optimized structures; all *ab initio* energies are from single point energies at EFP geometries. <sup>d</sup> Energies relative to symmetric system molecule-pair reactant to aid comparison of barrier heights and reaction energies.

As the number of water molecules increases, the number of stationary points on the potential energy surface will increase rapidly. One advantage of the Menshutkin reaction is that the

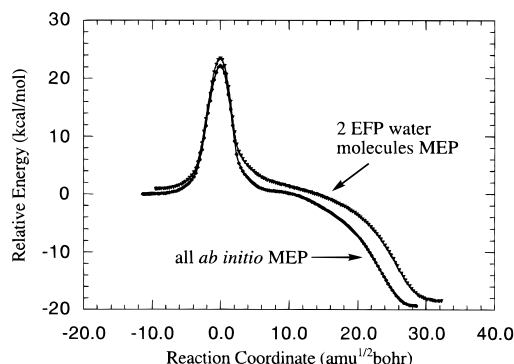


**Figure 5.** Minimum energy paths (MEPs) for the Menshutkin reaction (R3) with two water molecules. The bottom curve was calculated all *ab initio*; the top curve was calculated with two EFP water molecules.

**TABLE 4:  $\Delta H(0$  K),  $\Delta H(298.15$  K), and  $\Delta G(298.15$  K) of Activation and Reaction (in kcal/mol) Calculated at the RHF/DZVP Level for the Menshutkin Reaction (R3) with 0, 2, and 8 Solvating Water Molecules**

	0 waters	2 <i>ab initio</i> waters	2 EFP waters	8 EFP waters
DH(0 K)				
M-P React.	0.0	0.0	0.0	0.0
T.S.	36.2	24.3	24.4	20.3
I-P Prod.	-0.6	-14.2	-13.8	-25.3
DH(298.15 K)				
M-P React.	0.0	0.0	0.0	0.0
T.S.	34.7	22.6	23.1	19.6
I-P Prod.	-2.4	-16.1	-15.7	-27.1
DG(298.15 K)				
M-P React.	0.0	0.0	0.0	0.0
T.S.	40.6 <sup>a</sup>	28.3	27.7	22.8
I-P Prod.	2.8 <sup>b</sup>	-10.2	-10.3	-21.9

<sup>a</sup> T.S.(1). <sup>b</sup> I-P Prod.(2) (see Figures 2 and 3).

solute molecules must be essentially collinear in the transition state. The approach is therefore the same as with two waters: attempt to find the lowest energy transition state and follow MEPs to determine reactants and products. It must be stressed, however, that this approach does not ensure that global minima are found.

The starting points for the four- and six-water systems were obtained by addition of water molecules to the transition state found previously for the two-water system. This was done in a symmetric fashion, resulting in a transition state for the four-water system which is essentially  $C_{3v}$ , and a six-water transition state which possesses a nearly  $C_3$  axis of rotation (see Figures 6 and 7).

The effect of the presence of four EFP waters is a reduction of the molecule-pair reactant-transition state barrier by 8.8 kcal/mol compared to that in the two EFP water case (see Table 3). The resulting barrier is only 13.7 kcal/mol. Figure 6 shows that the four-water transition state occurs earlier than the two-water transition state as expected. The exothermicity of the ion-pair product is increased by 15.2 kcal/mol, compared to the two-water case; with four waters it is exothermic by 34.6 kcal/mol relative to the molecule-pair reactant. Again the waters enable the barrierless migration of the Br to the ammonium group where it is hydrogen-bonded to ammonium hydrogen and two water hydrogens.

The six-water system based on the approximately  $C_3$  transition state does not follow the predicted trend based on the two- and four-water results. The molecule-pair reactant-transition state

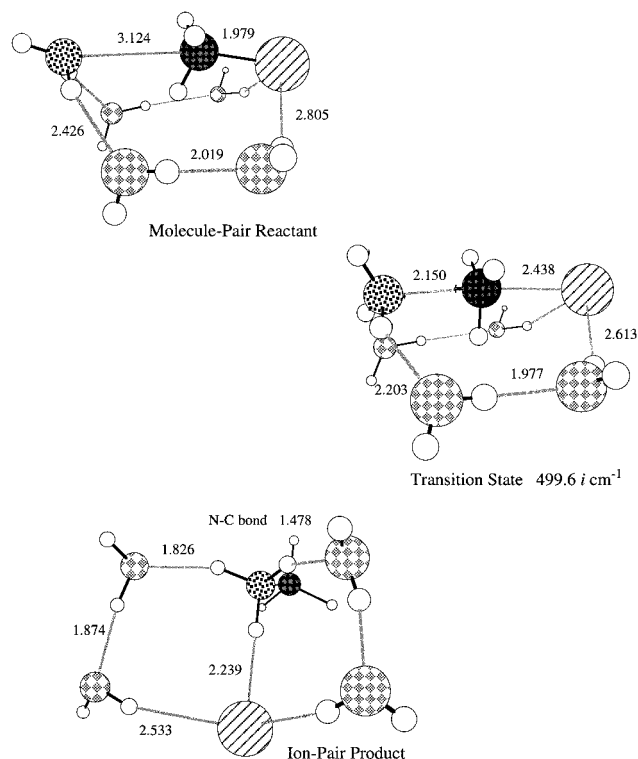


**Figure 6.** RHF/DZVP stationary point structures (symmetric system) on the potential energy surface of the Menshutkin reaction (R3) with four EFP water molecules. Bond lengths are in angstroms; only selected symmetry unique bond lengths are shown. Arrows in transition state indicate displacements in the imaginary normal mode.

barrier has increased by 8.4 kcal/mol compared to the four-water case, and the energy of the ion-pair product has increased by 14.0 kcal/mol. This can be explained using the structures in Figure 7. The transition state appears earlier in the reaction than in the two- and four-water cases, as one would expect. The larger barrier, then, must be explained by preferential stabilization, by the water molecules, of the molecule-pair reactant relative to the transition state. It appears that six waters allow more flexibility in the molecule-pair reactant which no longer has a collinear arrangement of  $\text{NH}_3$  and  $\text{CH}_3\text{Br}$  as it did in the two- and four-water cases. Presumably, this added flexibility made possible by the solvent is the reason for preferential stabilization of the molecule-pair reactant over the transition state. For the ion-pair product the opposite is true; the symmetric arrangement of waters has constrained  $\text{CH}_3\text{NH}_3^+$  and  $\text{Br}^-$  to a collinear arrangement, no longer allowing the *barrierless* migration of Br to the ammonium hydrogen. The result is a product less favorable energetically (see Table 3). It is probable that there exists a path corresponding to bromide migration to an ammonium hydrogen. However, a single transition state linking the "symmetric" product and a low-energy species with a bromide-ammonium hydrogen interaction could not be found. Instead, the transition state found which connects to the "symmetric" product ( $\sim 1$  kcal/mol higher in energy) leads only to a slight rearrangement in the solvent. This suggests the path to bromide migration is complex with multiple transition states and intermediates.

To determine if there are more energetically favorable arrangements of the water molecules in the transition states, alternative nonsymmetric structures were explored. Figure 8 shows a nonsymmetric four water transition state geometry and the molecule-pair reactant and ion-pair product found by following the MEPs from this transition state. This results (Table

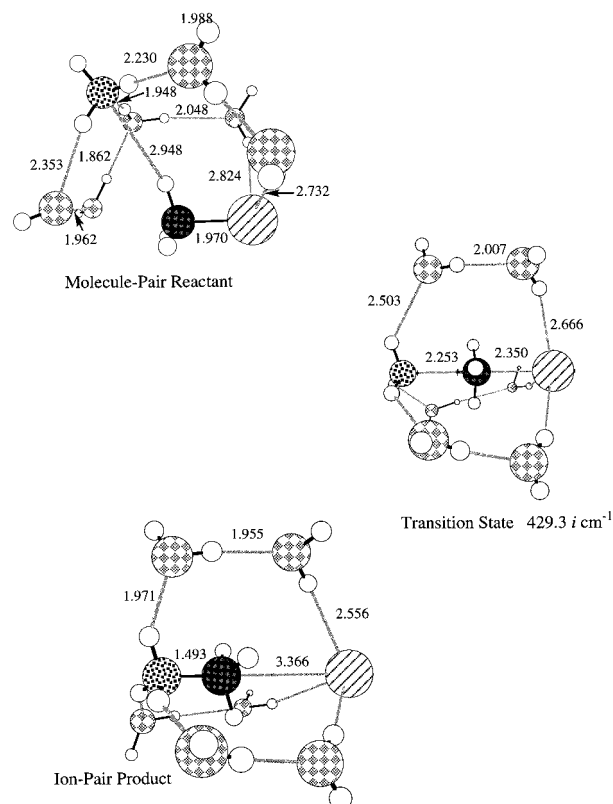


**Figure 7.** RHF/DZVP stationary point structures (symmetric T.S. and product) on the potential energy surface of the Menshutkin reaction (R3) with six EFP water molecules. Bond lengths are in angstroms; only selected symmetry unique bond lengths are shown. Arrows in transition state indicate displacements in the imaginary normal mode.

3) in an increase in the barrier to the transition state from the molecule-pair reactant, by 4.3 kcal/mol, to 18.0 kcal/mol and an increase in the energy of the ion-pair product relative to the molecule-pair reactant by 8.4 kcal/mol, to  $-26.2$  kcal/mol. In order to make a meaningful comparison, we must compare not only the barrier heights and relative energies of molecule-pair reactant and ion-pair product but also the relative energies of the symmetric and nonsymmetric cases. Figure 9 shows the two MEPs for these four-water systems. Both curves are plotted relative to the energy of the molecule-pair reactant obtained from the nonsymmetric transition state (Figure 8). The plots show that the molecule-pair reactant obtained from the nonsymmetric transition state is  $\sim 4$  kcal/mol lower in energy than that obtained from the symmetric transition state, the transition states themselves are nearly isoenergetic, and the ion-pair product obtained from the symmetric transition state is  $\sim 4$  kcal/mol lower in energy than that obtained from the nonsymmetric transition state. The actual path for the four-water case, then, must crossover between the unsymmetrical and symmetrical paths shown in Figure 9.

The six-water nonsymmetric system (see Figure 10) has a transition state with a ring, or crown, of five hydrogen-bonded waters, with two of the waters also hydrogen-bonded to bromine. The sixth water is outside the ring but is hydrogen-bonded to it and also to one of the  $\text{NH}_3$  hydrogens. Table 3 shows that in this nonsymmetric six-water system the barrier from molecule-pair reactant to transition state is 16.0 kcal/mol, a reduction of 6.1 kcal/mol compared to the symmetric system barrier. The energy of ion-pair product is  $-29.1$  kcal/mol relative to the molecule-pair reactant, a decrease in energy of 8.5 kcal/mol relative to the symmetric system. The MEPs shown in Figure 11 are plotted relative to the molecule-pair reactant obtained

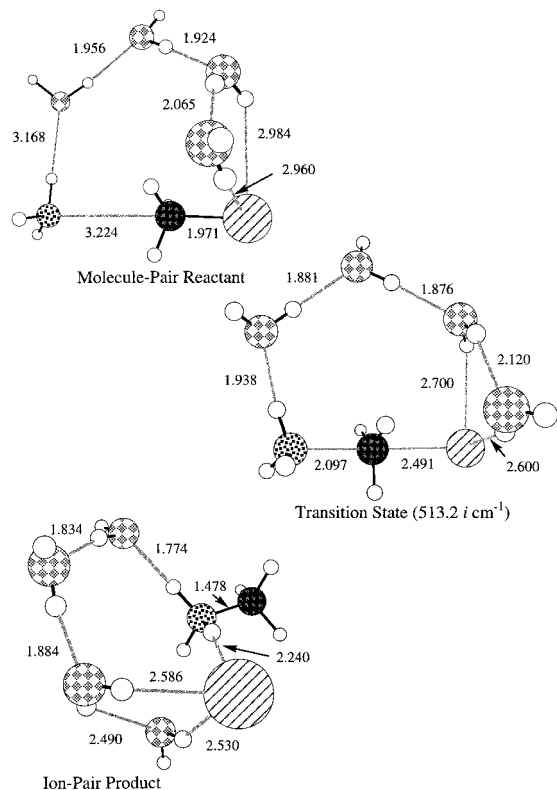


**Figure 8.** RHF/DZVP nonsymmetric stationary point structures on the potential energy surface of the Menshutkin reaction (R3) with four EFP water molecules. Bond lengths are in angstroms.

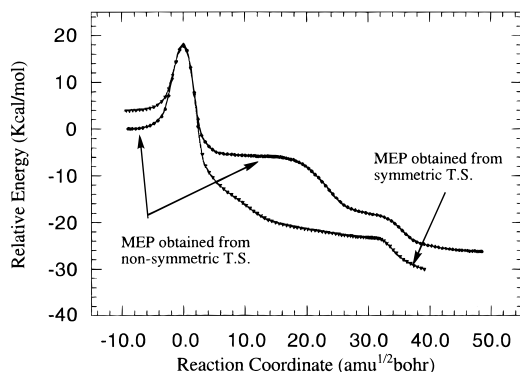


**Figure 9.** Minimum energy paths (MEPs) for the Menshutkin reaction (R3) with four EFP water molecules. One MEP was obtained from a symmetric transition state as the starting point; the other was obtained from a nonsymmetric transition state as the starting point. Energy points are relative to the lowest energy ion-pair reactant (obtained from nonsymmetric transition state).

from the nonsymmetric transition state. The two molecule-pair reactants are almost isoenergetic (there is a difference of only 0.9 kcal/mol). The nonsymmetric transition state, however, is considerably lower in energy than its symmetric counterpart (by 7.0 kcal/mol), and the corresponding ion-pair product is 9.4 kcal/mol lower in energy than the symmetric analog. The nonsymmetric surface is therefore clearly more favorable.

Returning to Table 3 and Figures 9 and 11, one may compare the most favorable four- and six-water systems to see that the four-water case is still slightly favored. This may mean that the increase in stabilization is not monotonic with the number of water molecules, or that more arrangements of solvent molecules must be considered. It is certainly likely that as the number of solvent molecules is increased, the number of possible structural arrangements also increases.

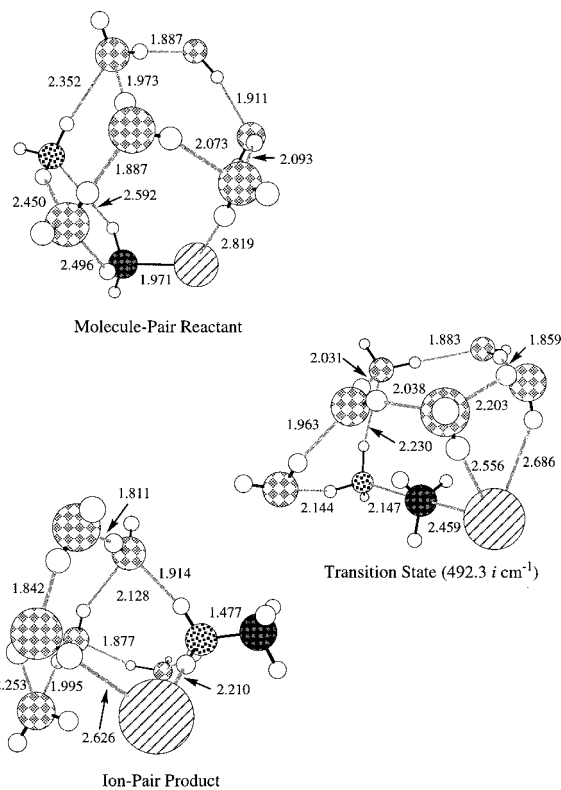


**Figure 10.** RHF/DZVP nonsymmetric stationary point structures on the potential energy surface of the Menshutkin reaction (R3) with six EFP water molecules. Bond lengths are in angstroms.

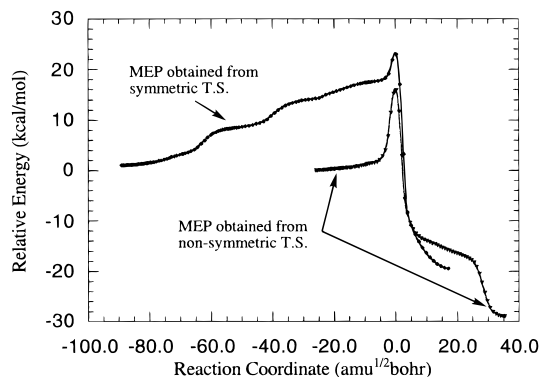


**Figure 11.** Minimum energy paths (MEPs) for the Menshutkin reaction (R3) with six EFP water molecules. One MEP was obtained from a symmetric transition state as the starting point; the other was obtained from a nonsymmetric transition state as the starting point. Energy points are relative to the lowest energy ion-pair reactant (obtained from nonsymmetric transition state).

To assess the accuracy of the EFP method for these four- and six-water cases all *ab initio* RHF/DZVP single-point energies were calculated at the EFP geometries. Again agreement is found to be excellent (see Table 3). For the four-water case, relative energies are found to agree to within 0.7 kcal/mol and for the six-water case to within 2.7 kcal/mol.

**(d) Eight Waters.** The eight-water transition state was found to have five waters in a crown arrangement like that seen in the nonsymmetric six-water case, with the three remaining waters forming a chain along the underside of the collinear solute (see Figure 12). The molecule-pair reactant–transition state barrier is calculated to be 20.9 kcal/mol, and the ion-pair product energy is  $-30.9$  kcal/mol relative to the molecule-pair reactant (see Table 3). The transition state occurs earlier than that in the nonsymmetric six-water structure (see Figure 10);



**TABLE 5: All *ab initio* versus EFP Method Timings Taken from Calculations Carried out on an IBM RS6000/350<sup>a</sup>**

no. of solvating H <sub>2</sub> O's	no. of basis functions <sup>b</sup>	energy				energy + gradient					
		CPU		wall clock		CPU		wall clock		$\Delta(\text{wall clock})^d$	
		ab	EFP	ab	EFP	ab	EFP	ab	EFP	ab	EFP
0 H <sub>2</sub> O	94	266 (1416)		596 (1434)		556 (1706)		889 (1727)			
2 H <sub>2</sub> O	144	1155 (4493)	337 (1546)	3141 (4537)	817 (1561)	2012 (5348)	890 (2099)	4006 (5399)	1376 (2118)	3117 (3672)	487 (391)
4 H <sub>2</sub> O	194	3334 (15927)	366 (1603)	9905 (16052)	851 (1619)	5182 (17765)	1166 (2400)	11768 (17905)	1658 (2422)	7762 (12506)	282 (304)
6 H <sub>2</sub> O	244		416 (23008)		964 (1877)		1493 (2954)		2054 (26684)		396 (8779)
8 H <sub>2</sub> O	294		430 <sup>c</sup> (39577)		942 <sup>c</sup> (1764) <sup>c</sup>		1752 (3082)		2275 (45029)		221 (18345)

<sup>a</sup> Bracketed times are for direct SCF; others are for conventional SCF. All times are given in seconds. <sup>b</sup> For EFP no. of basis functions always 94. <sup>c</sup> Took 1 less SCF cycle than previous calculations. <sup>d</sup> Time difference resulting from each addition of two water molecules.

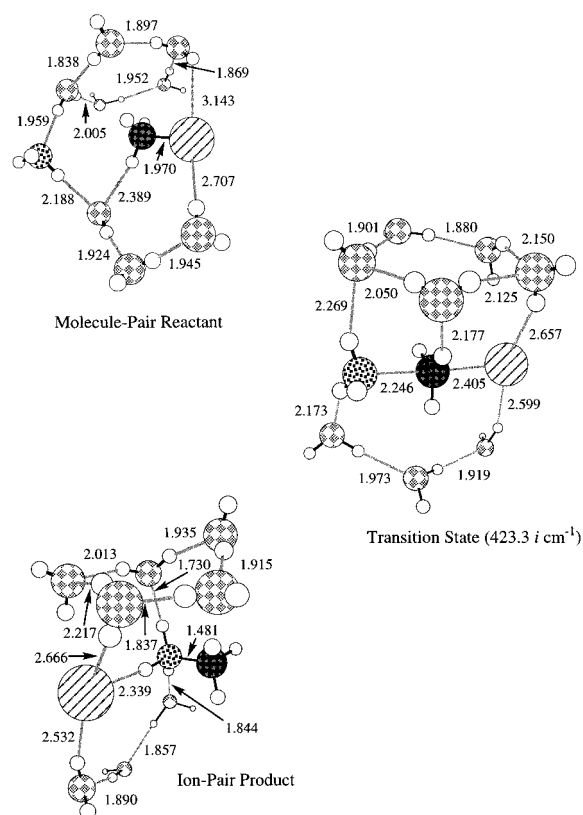


**Figure 12.** RHF/DZVP stationary point structures on the potential energy surface of the Menshutkin reaction (R3) with eight EFP water molecules. Bond lengths are in angstroms.

however, the barrier height is  $\sim 4$  kcal/mol greater than that for the six-water nonsymmetric system. Apparently, there is more effective hydrogen bonding between the amine and waters in the reactant with eight solvating waters (compare the molecule-pair reactants in Figure 12 and 10). The ion-pair product retains the ammonium hydrogen-bromide interaction. Figure 13 shows the MEP for the eight-water system. Inclusion of ZPE, as well as thermal and entropy effects at 298.15 K (Table 4) gives a free energy of activation of 22.8 kcal/mol and a free energy of reaction of  $-21.9$  kcal/mol, the reactant complex once again being favored by these combined effects. The value of  $\Delta H(0 \text{ K})$  of activation (20.3 kcal/mol) (see Table 4) may be compared to the experimental activation energy for the iodide system in aqueous solution<sup>18</sup> (23.5 kcal/mol). No experimental data could be found for the bromide system.

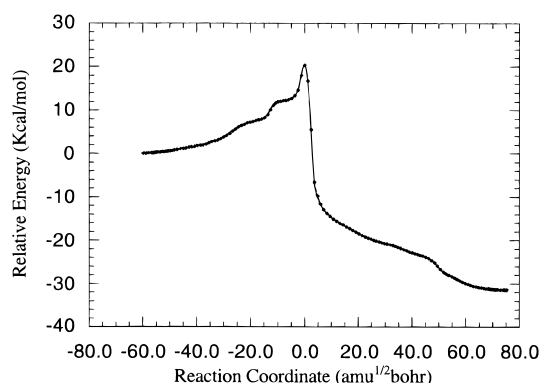


**Figure 13.** Minimum energy path (MEP) for the Menshutkin reaction (R3) with eight EFP water molecules. Energy points are relative to the ion-pair reactant.

It is important to note that for the 4-, 6-, and 8-water cases the number of stationary points on the potential energy surface will be very large. Therefore, the energetics shown in Tables 3 and 4 cannot be viewed as definitive. It is only possible to ensure that the most favorable geometric arrangements have been found by a systematic sampling of the phase space. To accomplish this would require methods such as molecular dynamics (MD), Monte Carlo (MC), simulated annealing (SA), or genetic algorithm (GA) approaches. These methods are presently being interfaced with the EFP method, and results using them will be reported in subsequent papers.

#### IV. Timings

The EFP method was developed to model solvent effects accurately and cheaply. We have demonstrated above the accuracy of the method. In order to demonstrate how inexpensive the EFP method is in comparison to corresponding all *ab initio* calculations, we present timings in Table 5.

The EFP method scales linearly with the number of water molecules; times required for the all *ab initio* calculations increase much more rapidly. For the eight-water case the time required for an all *ab initio* energy + gradient calculation is 14 times that required for the EFP method. Even more impressive is the fact that the time taken for the all *ab initio* calculation of the eight water system energy + gradient is 26 times that required for the zero water case, while the EFP time only increases by a factor of 2.

The last two columns in Table 5 show the increase in wall clock time required which results from each addition of two



water molecules to the calculation (these times do not continuously increase down the columns, with the increase in the number of water molecules, as the number of SCF cycles is not constant). Comparison of the *ab initio* and EFP  $\Delta$  (wall clock) times clearly demonstrates how inexpensive the addition of water molecules in the EFP method is relative to all *ab initio* calculations.

## V. Conclusions

We have tested the recently developed effective fragment potential (EFP) method,<sup>7–12</sup> for modelling solvent effects, on the ammonia plus methyl bromide Menshutkin reaction. The method accurately reproduces the all *ab initio* geometries and energetics (including entropy effects) for the reaction with two solvating water molecules. Comparison of EFP energetics with all *ab initio* single-point energies at the EFP geometries for four, six, and eight solvating waters also shows excellent agreement.

Calculations on the gas phase Menshutkin reaction confirm previous findings that a low-energy ion-pair product with the bromide anion hydrogen-bonded to an ammonium hydrogen exists with an energy of  $-4.7$  kcal/mol relative to the molecule-pair reactant at the RHF/DZVP level of theory, but the reaction barrier is very high, 34.0 kcal/mol. Dynamic electron correlation introduced through MP2 was found to have only a small effect on the gas phase potential energy surface. ZPE, thermal, and entropy effects at room temperature combined favor the reactant; with their inclusion the reaction barrier increases by 7.5 kcal/mol giving a free energy of activation of 40.6 kcal/mol and a reaction free energy of 2.8 kcal/mol.

With the addition of two EFP water molecules the barrier is reduced to 22.5 kcal/mol and the ion-pair product energy relative to the molecule-pair reactant is lowered to  $-19.4$  kcal/mol. Inclusion of ZPE, thermal, and entropy effects at 298.15 K gives a free energy of activation of 27.7 kcal/mol and a reaction free energy of  $-10.3$  kcal/mol. For eight solvating water molecules the barrier is 20.9 kcal/mol and the ion-pair product is lower in energy than the molecule-pair reactant by  $-30.9$  kcal/mol. Inclusion of ZPE, thermal, and entropy effects at 298.15 K gives a free energy of activation of 22.8 kcal/mol and a free energy of reaction of  $-21.9$  kcal/mol. All but one (symmetric six-water case) of the ion-pair products in the solvated systems examined contain the bromide anion–ammonium hydrogen interaction seen in the gas phase calculations.

The overall trend, as expected, is a decrease in the barrier height and an increase in the exothermicity as the number of water molecules is increased. However, it is clear that for 4, 6, 8, and more water molecules there will be many more possible geometric arrangements than those actually considered. In order to ensure that the most favorable geometric arrangements have been found for these systems (and systems with additional waters) it will be necessary to systematically sample the phase space with methods that are designed for this purpose.

The main purpose of this work has been to assess the EFP method for a challenging problem, not to study the effect of bulk water on the Menshutkin reaction (which gives truly separated ion products). We have, however, investigated the effect of small water clusters on this important reaction. Timings presented show the EFP method to be an inexpensive way to model *ab initio* solvation effects very accurately. Future work will use the EFP method together with sophisticated sampling

techniques to add many more water molecules to investigate bulk effects on the Menshutkin and other reactions.

**Acknowledgment.** This work was supported by a grant from the National Science Foundation (CHE-9633480). The calculations reported here were performed on IBM RS 6000 workstations generously provided by Iowa State University. The authors thank Dr. Jan Jensen for many informative discussions.

## References and Notes

- (1) Karelson, M.; Tamm, T.; Zerner, M. C. *J. Phys. Chem.* **1993**, *97*, 11901.
- (2) (a) Miertus, S.; Scrocco, E.; Tomasi, J. *Chem. Phys.* **1981**, *55*, 117. (b) Tomasi, J.; Persico, M. *Chem. Rev.* **1994**, *94*, 2027. (c) Cammi, R.; Tomasi, J. *J. Comput. Chem.* **1995**, *16*, 1449.
- (3) Schmidt, M. W.; Windus, T. L.; Gordon, M. S. *J. Am. Chem. Soc.* **1995**, *117*, 7480.
- (4) (a) Cramer, C. J.; Truhlar, D. G. *Reviews in Computational Chemistry*; Boyd, D. B., Lipkowitz, K. B., Eds.; VCH: New York, 1995; Vol. 6. (b) Truong, T. N.; Truong-Thai, T.; Stefanovich, E. V. *J. Phys. Chem.* **1997**, *107*, 1881. (c) Stefanovich, E. V.; Truong, T. N. *Chem. Phys. Lett.* **1995**, *244*, 65. (d) Davidson, M. M.; Hillier, I. H.; Vincent, M. A. *Chem. Phys. Lett.* **1995**, *246*, 536. (e) Wiberg, K. B.; Rablen, P. R.; Rush, D. J.; Keith, T. A. *J. Am. Chem. Soc.* **1995**, *117*, 4261. (f) Giesen, D. J.; Cramer, C. J.; Truhlar, D. G. *J. Phys. Chem.* **1995**, *99*, 7137. (g) Giesen, D. J.; Storer, J. W.; Cramer, C. J.; Truhlar, D. G. *J. Am. Chem. Soc.* **1995**, *117*, 1057. (h) Amovilli, C.; Mennucci, B.; Floris, F. M. *J. Phys. Chem. B* **1998**, *102*, 3023.
- (5) Jensen, J. H.; Gordon, M. S. *J. Am. Chem. Soc.* **1995**, *117*, 8159.
- (6) (a) Gao, J. *Acc. Chem. Res.* **1996**, *29*, 298. (b) de Vries, A. H.; van Duijnen, P. T.; Juffer, A. H.; Pullman, A. C.; Dijkman, J. P.; Merenga, H.; Thole, B. T. *J. Comput. Chem.* **1995**, *16*, 37. (c) Thompson, M. A.; Glendening, E. D.; Feller, D. F. *J. Phys. Chem.* **1994**, *98*, 10465. (d) Luzhkov, V.; Warshel, A. *J. Comput. Chem.* **1992**, *13*, 199. (e) Field, M. J.; Bash, P. A.; Karplus, M. *J. Comput. Chem.* **1990**, *11*, 700.
- (7) Jensen, J. H.; Day, P. N.; Gordon, M. S.; Basch, H.; Cohen, D.; Garmer, D. R.; Krauss, M.; Stevens, W. J. In *Modeling the Hydrogen Bond*; Smith, D. A., Ed.; ACS Symposium Series 569; American Chemical Society: Washington, DC, 1994; p 139.
- (8) Day, P. N.; Jensen, J. H.; Gordon, M. S.; Webb, S. P.; Stevens, W. J.; Krauss, M.; Garmer, D. R.; Basch, H.; Cohen, D. *J. Chem. Phys.* **1996**, *105*, 1969.
- (9) Merrill, G. N.; Gordon, M. S. *J. Phys. Chem. A* **1998**, *102*, 2650.
- (10) Chen, W.; Gordon, M. S. *J. Chem. Phys.* **1996**, *105*, 11081.
- (11) Krauss, M.; Webb, S. P. *J. Chem. Phys.* **1997**, *107*, 5771.
- (12) Day, P. N.; Pachter, R. *J. Chem. Phys.* **1997**, *107*, 22.
- (13) (a) Menshutkin, N. Z. *Phys. Chem.* **1890**, *5*, 589. (b) Menshutkin, N. Z. *Phys. Chem.* **1890**, *6*, 41.
- (14) McMurry, J. *Organic Chemistry*; Brooks/Cole Publishing Co.: New York, 1984; p 933.
- (15) Solà, M.; Lledós, A.; Duran, M.; Bertrán, J.; Abboud, J. M. *J. Am. Chem. Soc.* **1991**, *113*, 2873.
- (16) Gao, J.; Xia, X. *J. Am. Chem. Soc.* **1993**, *115*, 9667.
- (17) Jorgensen, W. L.; Chandrasekhar, J.; Madura, J. D.; Impey, R. W.; Klein, M. L. *J. Chem. Phys.* **1983**, *79*, 926.
- (18) Okamoto, K.; Fukui, S.; Shingu, H. *Bull. Chem. Soc. Jpn.* **1967**, *40*, 1920.
- (19) Maran, U.; Pakkanen, T. P.; Karelson, M. *J. Chem. Soc., Perkin Trans.* **1994**, *2*, 2445.
- (20) Maran, U.; Karelson, M.; Pakkanen, T. P. *J. Mol. Struct. (Theochem)* **1997**, *397*, 263.
- (21) (a) Binkley, J. S.; Pople, J. A. *Int. J. Quantum Chem.* **1975**, *9*, 229. (b) Krishnan, R.; Pople, J. A. *Int. J. Quantum Chem.* **1978**, *14*, 91.
- (22) Dunning, T. H.; Hay, P. J. In *Methods of Electronic Structure Theory*; Schaefer III, H. F., Ed.; Plenum Press: New York, 1977; Chapter 1, pp 1–27.
- (23) Binning, R. C.; Curtiss, L. A. *J. Comput. Chem.* **1990**, *11*, 1206.
- (24) Schmidt, M. W.; Baldridge, K. K.; Boatz, J. A.; Jensen, J. H.; Koseki, S.; Matsunaga, N.; Gordon, M. S.; Nguyen, K. A.; Su, S.; Windus, T. L.; Elbert, S. T.; Montgomery, J.; Dupuis, M. *J. Comput. Chem.* **1993**, *14*, 1347.
- (25) Gonzalez, C.; Schlegel, H. B. *J. Phys. Chem.* **1990**, *94*, 5523. Step sizes between 0.10 and 0.30 bohr amu<sup>1/2</sup> were used.